A MICRO-MACRO EVALUATION OF THE VERTEBRAL BONY ENDPLATE PERMEABILITY BASED ON COMPUTATIONAL FLUID DYNAMICS

[1]Andrea Malandrino, [2]Christian Hellmich, [1]Jérôme Noailly and [1]Damien Lacroix
[1]Institute for Bioengineering of Catalonia, Barcelona, Spain; email: amalandrino@ibecbarcelona.eu, web: www.biomechanics.es,
[2]Institute for Mechanics of Materials and Structures. Vienna, Austria,

SUMMARY

The intrinsic permeability is an important parameter that describes the resistance of a porous structure to fluid flow. It has a key role in poroelastic finite element models of spinal segments, especially at the vertebral endplate, i.e. the interface between intervertebral disc and vertebra. In the understanding of the properties of the complex endplate system, an explicit evaluation for permeability of subchondral bone is missing. Thus, a new method was proposed to evaluate the intrinsic permeability of the bony endplate. μCT-based reconstructions of the bony endplate from a lumbar vertebra were analyzed using computational fluid dynamics, and the intrinsic permeability and porosity of the structure were calculated. Results showed that the permeability did not depend on the fluid flow direction, and was statistically similar for both the superior and inferior endplates. Permeability values varied within the range of trabecular bone, while porosity values were lower than trabecular bone characteristic values. Finally, intrinsic permeability correlated well with porosity through the Kozeny-Karman model, which offers perspectives for parametric studies involving degenerative or age-related changes at the disc-bone interface.

INTRODUCTION

Resistance to fluid flow is a key property of the interface between intervertebral disc and vertebrae, which strongly influences spinal segment biomechanics and transport of nutrients [1]. A parameter that describes such a resistance is the permeability, which is of central importance in poroelastic modeling of the intervertebral disc [2]. Due to extremely reduced thickness of the subchondral bone at the disc interface, experimental techniques were not able to explicitly evaluate permeability of the bony endplate portion at the macroscopic level. As such, permeability values extracted from permeation experiments as well as the flow direction-dependent difference of the results [1,3] were likely more representative of the adjacent cartilaginous layer that consolidates more and is less permeable than bone. However with aging, degeneration and/or endplate calcification, the cartilage endplate becomes thinner [3], increasing the importance of the subchondral bone permeability. A direct evaluation for subchondral bone permeability and porosity would therefore provide input poroelastic parameters for modeling degeneration/calcification at the endplates.

Micro-computer tomography (μCT) offers a bone structural mapping from which it is possible to simulate the permeation of fluid and thus evaluate the resistance to fluid flow. Thus, by using μCT-based finite element models, the aim of this study was to calculate the permeability of the bony endplate through computational fluid dynamics (CFD) analyses.

METHODS

μCT scans (XtremeCT, Scanco Medical AG, Switzerland) of a L1 human vertebra were used. The voxel resolution was 12 μm. 3D parallelepiped (2.5 x 2.5 x 3 mm^3) models were generated for CFD analyses using mixed hexahedral and tetrahedral finite volumes with ScanIP© (Simpleware Ltd.). The models considered a squared cross section (2.5x2.5 mm^2) of the bony endplate. The third dimension was aligned with the superior-inferior direction and coincided with the fluid flux direction. Trabecular bone was removed in order to leave the complete endplate part in the model. Thus, the thickness of the porous zone was variable from sample to sample, depending on the particular morphology observed during the image segmentation (Fig. 1). Endplate permeation was then simulated. A mass flux boundary inlet of 10^{-5} kg/s was applied at a distance of approximately 2 mm from the endplate. The pressure at the outlet cross section was null. Flow-in (from vertebra to disc) analyses were performed on 11 parallelepipeds from the inferior part of the vertebra and 11 from the superior one using FLUENT© CFD software. Flow-out (from disc to vertebra) analyses were also performed on four parallelepipeds from the superior part and four from the inferior one. The macroscopic permeability was evaluated with the Darcy relation

$$K = \frac{Q_{in} L}{\rho A \Delta P} = \frac{Q_{in} L}{\rho A (P_{in} - P_{out})}$$

where A is the cross sectional area, K is the hydraulic permeability, Q_{in} is the mass flux applied at the inlet, ρ is the fluid density and L is the distance between the two sections where the pressures P_{in} and P_{out} were computed. The intrinsic permeability, k, independent of the particular fluid simulated was calculated from K and the dynamic viscosity, ν:

$$k = K\nu$$

Porosity was evaluated for each sample by dividing the segmented fluid volume within the endplate by the total volume of fluid-filled structure. Results were statistically analyzed with Minitab® (Minitab Inc.) to screen out the effect of location (superior vs. inferior) and flow direction (in vs. out).

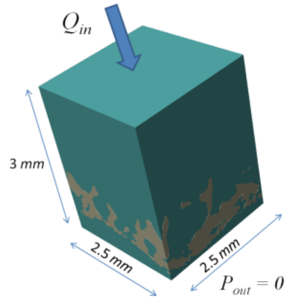

Figure 1: Sketch of the 3D model used for CFD analyses (flow-in case).

RESULTS AND DISCUSSION

No statistically significant differences were found between intrinsic permeability values from the superior and inferior endplates (p=0.19). The mean value for the superior endplate was 10.7×10^{-10} m^2 while for the inferior endplate, the value was 6.74×10^{-10} m^2 (Table 1). The average intrinsic permeability value for both superior and inferior parallelepipeds was 8.73×10^{-10} m^2. No statistically significant differences were found between flow-in and flow-out permeability (Paired T-test, p=0.443).

The porosity was also not statistically different between inferior and superior endplates (p=0.291), the mean global value being 64%. A positive correlation was found between the permeabilities and porosities pooled for superior and inferior endplate by using a Kozeny-Carman model (R^2=0.79) of the type $k = \frac{c\phi^{\alpha}}{S_V^2}$, where S_V is the specific surface, i.e. the internal surface of the pores per unit volume of the solid matrix [4].

	Permeability [$\times 10^{-10}$ m^2]	Porosity [%]
Superior	10.7 ± 7.10	65.1 ± 7.4
Inferior	6.74 ± 6.77	62.9 ± 7.1

Table 1: Permeability and porosity values found and relative standard deviations.

The range of intrinsic permeabilities, *k*, found in this study (1.16×10^{-10} to 2.73×10^{-9} m^2) can be compared with previous measurements on trabecular bone (2.68×10^{-11} to 2.00×10^{-8} m^2) [5], whereas it is out of the range of values found for cortical bone (5×10^{-15} to 6.35×10^{-13} m^2) [4]. However, the mean porosity found for the endplate was lower than the characteristic value usually taken for trabecular bone and higher than that of cortical bone, i.e. 80% and 0.05%, respectively [6]. This supports the idea that the vascular openings present in the endplate subchondral bone are specialized for both the exchange of nutrients between vertebrae and intervertebral discs, and the removal of disc waste products [7]. Therefore, endplate permeability could be an important parameter to monitor for the understanding of intervertebral disc degeneration in case of severe subchondral bone calcification.

The non-correlation between fluid flow-in and flow-out in the present study confirms that the observed dependency in experiments [1,3] should be attributed only to cartilaginous endplate and not to subchondral bone [1]. The correlation found between porosity and permeability, together with future studies using micro-to macro homogenization approaches, could be useful to parametrically explore the disc transport and biomechanics in spinal segments as a function of the subchondral bone calcification state.

To our knowledge, this is the first study that attempts an explicit evaluation of the subchondral bone permeability without associating it to the cortical or trabecular bone. Also, the proposed method to compute the macroscopic permeability excludes a possible biasing from the cartilaginous part of the interface disc-vertebra.

CONCLUSIONS

The results from this CFD-based evaluation of the macroscopic permeability of the vertebral endplate bone showed that bony endplate permeability is comparable to that of trabecular bone. No influences of the vertical location and fluid flow direction were found. The values of permeability and porosity obtained in this study are relevant for modeling purposes and may be useful in the future to improve our understanding of the degenerative changes occurring at the disc-bone interface.

ACKNOWLEDGEMENTS

Financial funding is acknowledged from the European Commission (NMP3-LA-2008-213904) and the Spanish Ministry of Science and Innovation (Acción Integrada AT2009-002 and FPU pre-doctoral fellowship AP2008-03317).

The authors are also grateful to Heinz Redl and Karl Kropik from the Austrian Center for Tissue Engineering and Ludwig Boltzmann Institute for Experimental and Clinical Traumatology, for providing a μCT data set of a human vertebra.

REFERENCES

1. Ayotte D C, et al., *Journal of Orthopaedic Research.* **19**:1073-1077, 2001.
2. Malandrino A, et al., *Journal of Biomechanics.* **42**:2780-2788, 2009.
3. Accadbled F, et al., *Spine.* **33**:312-619, 2008.
4. Cowin. *Bone Mechanics Handbook*, CRC press, Boca Raton, Florida, 2001.
5. Nauman E A, et al., *Annals of Biomedical Engineering.* **27**:517-524, 1999.
6. Recker, R R, *Bone Histomorphometry: Techniques and Interpretation*, CRC Press, Boca Raton, Florida, 1983.
7. Benneker L M, et al., *Spine.* **30**:167-173, 2005.